The development pathway for $CD103^+CD8^+$ tissue-resident memory T cells of skin

Laura K. Mackay[1,5], Azad Rahimpour[1,5], Joel Z. Ma[1,5], Nicholas Collins[1], Angus T. Stock[1], Ming-Li Hafon[1], Javier Vega-Ramos[1], Pilar Lauzurica[2], Scott N. Mueller[1], Tijana Stefanovic[3], David C. Tscharke[3], William R. Heath[1], Michael Inouye[1,4], Francis R. Carbone[1,6] & Thomas Gebhardt[1,6]

Nature Immunology: doi:10.1038/ni.2744

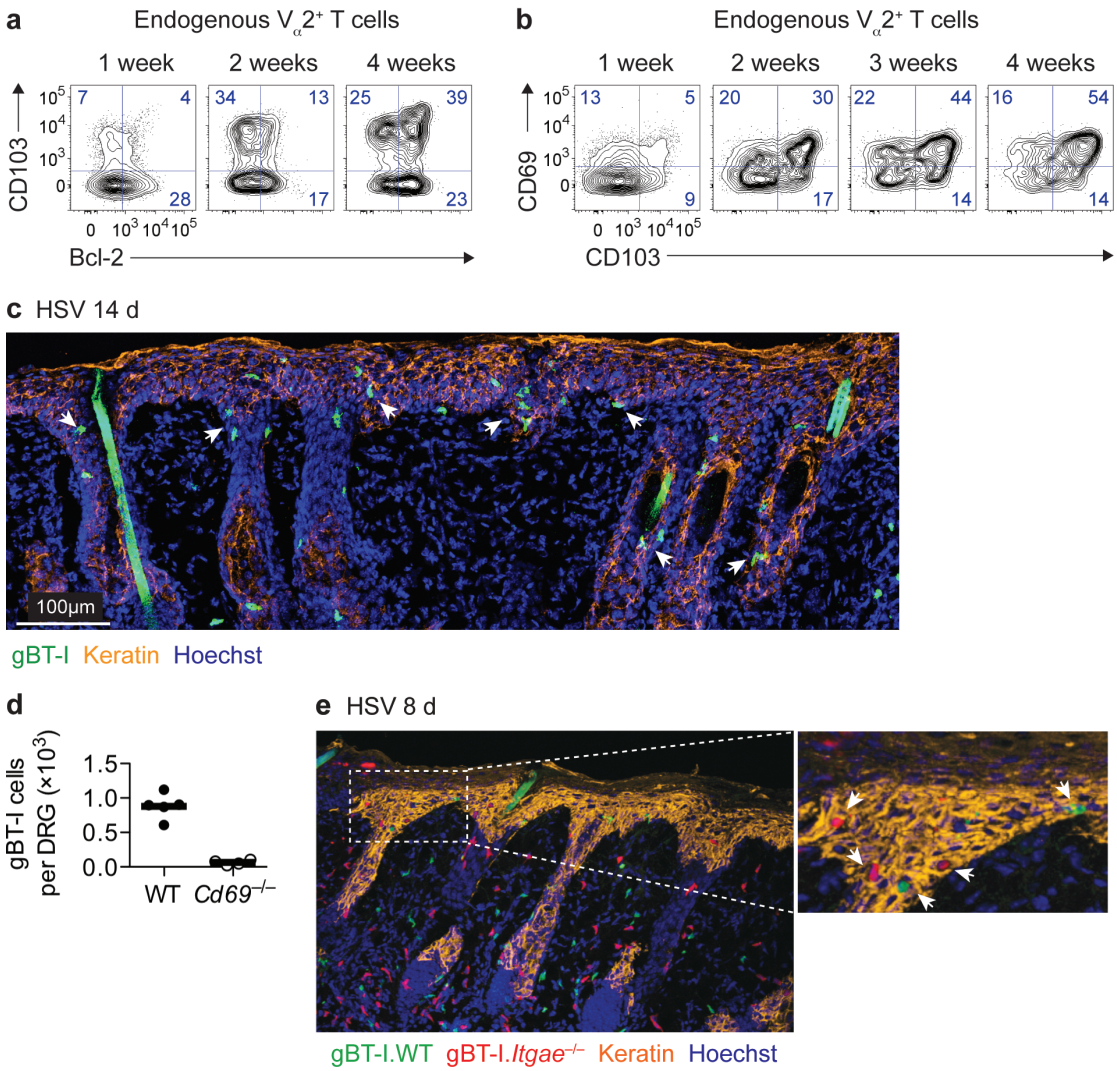

Supplementary Figure 1. Phenotype and anatomical localization of T_{RM} cells. (**a**,**b**) Analysis of CD103, Bcl-2 and CD69 expression by endogenous $V_\alpha2^+$ T cells in skin at the indicated times p.i. Plots are gated on $V_\alpha2^+$ CD45.2$^+$ cells; numbers indicate the percentage of events in the respective gates. Data representative of 2–3 experiments. (**c**) Mice received naïve gBT-I.GFP cells prior to HSV infection. Arrows indicate examples of gBT-I.GFP cells in the epidermis and hair follicle epithelium 14 d p.i. Photo representative of >5 experiments. (**d**) Wild-type (WT) and *Cd69*$^{-/-}$ gBT-I cells were transferred into WT mice prior to HSV infection. Enumeration of gBT-I cells in dorsal root ganglia (DRG) 30 d p.i. Data from one experiment (*n* = 5 mice/group). (**e**) WT (GFP-expressing, green) and *Itgae*$^{-/-}$ (DsRed-expressing, red) gBT-I cells were co-transferred into WT mice prior to HSV infection. Microscopy of skin 8 d p.i. Staining with anti-keratin antibody to delineate the epidermis and hair follicle epithelium. Arrows in insert indicate gBT-I cells in the epidermis. Photo representative of *n* = 3 mice analyzed.

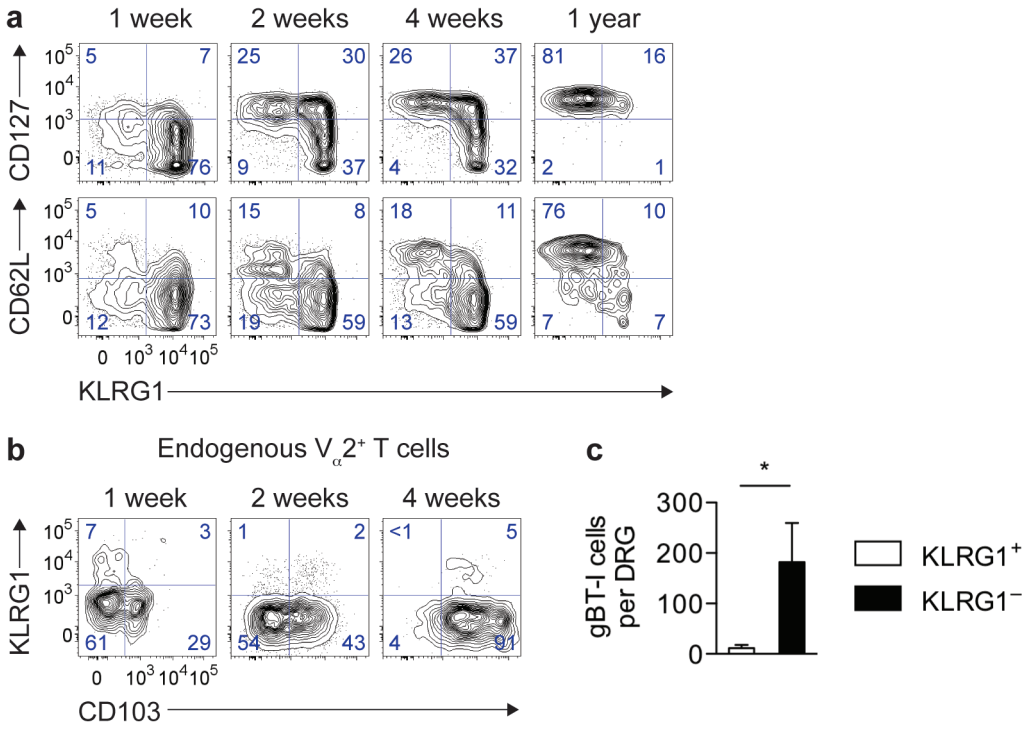

Supplementary Figure 2. Development of virus-specific CD8$^+$ memory T cells after HSV-1 skin infection. (**a**) Mice received naïve gBT-I cells prior to infection. Analysis of CD62L, CD127 and KLRG1 expression by gBT-I cells in the spleen at different time points after infection. Plots are gated on V$_\alpha$2$^+$CD45.2$^+$CD45.1$^+$ cells and are representative of *n* = 4–8 mice/time point. Numbers indicate the percentage of events in the respective gates (as in **b**). (**b**) Analysis of CD103 and KLRG1 expression by endogenous V$_\alpha$2$^+$ T cells in skin at the indicated times p.i. Plots are gated on V$_\alpha$2$^+$CD45.2$^+$ cells and are representative of 3 experiments (*n* = 12 mice/time point). (**c**) Effector gBT-I cells were sorted into KLRG1$^+$ and KLRG1$^-$ subsets from spleens of infected mice (6 d p.i.) and transferred into infected recipients (4 d p.i.). Enumeration of CD103$^+$ gBT-I cells in dorsal root ganglia (DRG) 3 weeks p.i. Data from 3 experiments (*n* = 12 mice/group); *, $P < 0.05$ by two-tailed Mann-Whitney test.

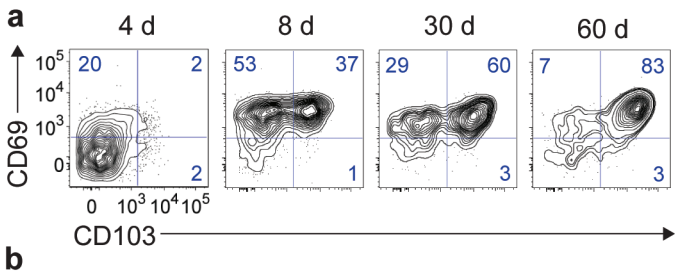

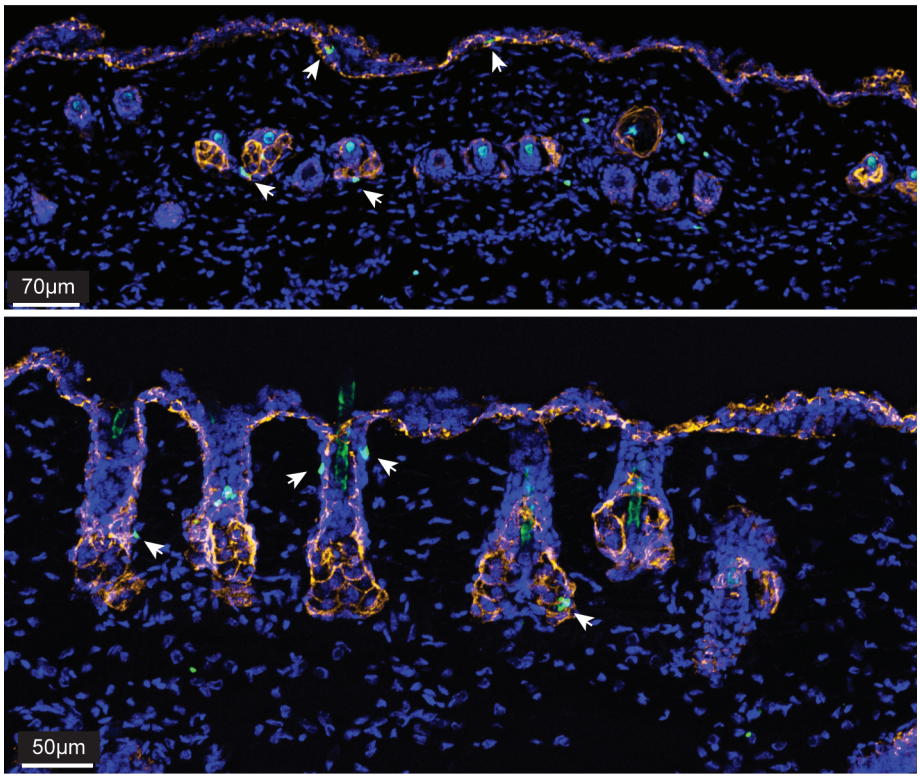

gBT-I.GFP Keratin Hoechst

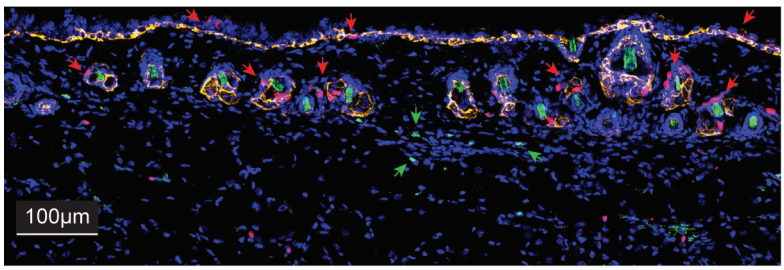

gBT-I (Ctrl) gBT-I (+PTx) Keratin Hoechst

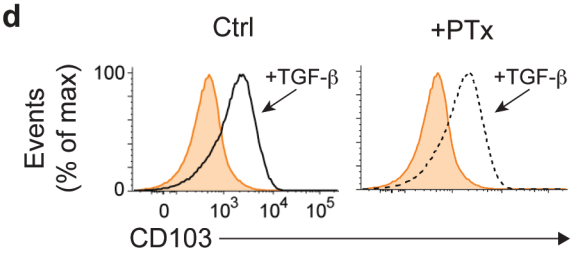

Nature Immunology: doi:10.1038/ni.2744

Supplementary Figure 3. Epidermal localization of CD8$^+$ T cells after intradermal transfer. (**a**) CD103 and CD69 expression by gBT-I cells in skin at the indicated times after *in vitro* activation by gB peptide-coated splenocytes and intradermal transfer. Plots are gated on Vα2$^+$CD45.2$^+$CD45.1$^+$ cells and are representative of 2–3 experiments (*n* = 6–12 mice/time point). Numbers indicate the percentage of events in the respective gates. (**b**) *In vitro* activated gBT-I.GFP cells were transferred into the skin by intradermal injection. Microscopy of skin 30 d after transfer. Staining with anti-keratin antibody to denote epithelium in the epidermis and hair follicles. Arrows indicate examples of gBT-I.GFP cells (green). Photos (2 examples shown) are representative of 2 experiments. (**c**) *In vitro* activated gBT-I cells were left untreated (Ctrl, DsRed-expressing, red) or treated with PTx (+PTx, GFP-expressing, green) and co-transferred into mice by intradermal injection. Microscopy of skin 4 weeks after transfer; anti-keratin staining denotes the epidermal layer and hair follicle epithelium. Red arrows indicate control cells in the epithelium, green arrows indicate PTx-treated cells in the dermis. Photos representative of 2 experiments. (**d**) *In vitro* activated gBT-I cells were untreated (Ctrl) or treated with PTx (+PTx). Analysis of CD103 expression following subsequent *in vitro* incubation of the cells in the presence (solid or dashed black lines, as indicated) or absence (orange area) of TGF-β (5 ng/ml; 24 hours). Plots are gated on Vα2$^+$CD45.2$^+$CD45.1$^+$ cells and are representative of 2 experiments.

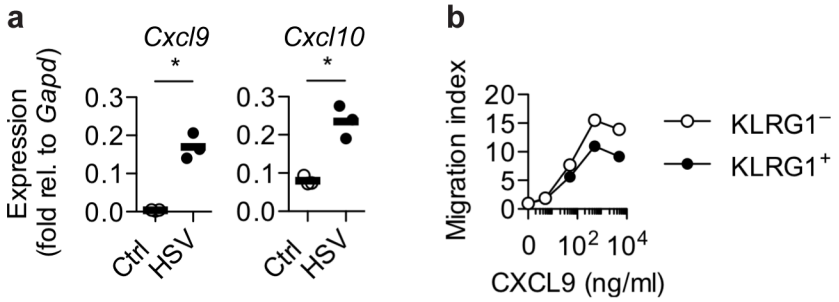

Supplementary Figure 4. Chemokine expression in skin and *ex vivo* migration of KLRG1$^+$ and KLRG1$^-$ effector cells. (**a**) mRNA expression for genes encoding CXCL9 and CXCL10 in CD45.2$^-$EpCAM$^+$ keratinocytes sorted from naïve (Ctrl) or HSV-infected skin (d 6 p.i.). Data pooled from 3 independent experiments (represented by individual symbols). *, $P < 0.05$ by two-tailed paired *t*-test. (**b**) *Ex vivo* migration towards CXCL9 gradients by KLRG1$^+$ (closed symbols) and KLRG1$^-$ (open symbols) gBT-I cells enriched from spleens 7 d after HSV skin infection (cells pooled from $n = 5$ donor mice).

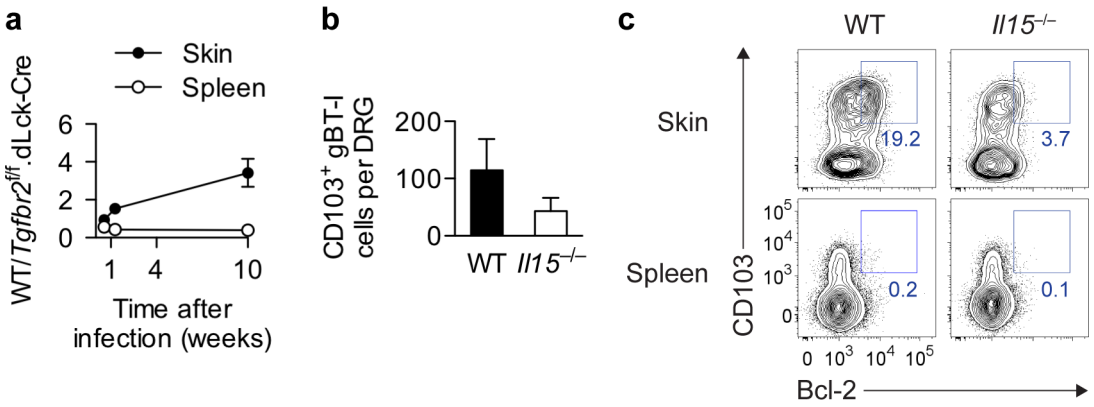

Supplementary Figure 5. Requirement of TGF-β receptor and IL-15 signaling in the development of CD103$^+$ T_{RM} cells. (**a**) Wild-type (WT) and TGF-R-deficient (*Tgfbr2f/f*.dLck-Cre) OT-I cells were activated by culture with ovalbumin peptide-coated splenocytes and transferred into the skin by intradermal injection. Depicted are the ratios of WT relative to *Tgfbr2f/f*.dLck-Cre cells in the skin and spleen at the indicated times after transfer. Data representative of 2 experiments (*n* = 3–4 mice/group). (**b**,**c**) Effector gBT-I cells were enriched from spleens of WT mice (6 d p.i.) and transferred into infected (4 d p.i.) WT or *Il15*$^{-/-}$ recipient mice. (**b**) Enumeration of CD103$^+$ gBT-I cells in dorsal root ganglia (DRG) 4 wks p.i. Data from one experiment with *n* = 5 mice/group. (**c**) CD103 and Bcl-2 expression by gBT-I cells in WT and *Il15*$^{-/-}$ mice (11 d p.i.). Plots are gated on V_a2^+CD45.2$^+$CD45.1$^+$ cells; numbers depict percentages of events in the respective gates. Data are representative of 2 experiments (*n* = 8 mice/group).

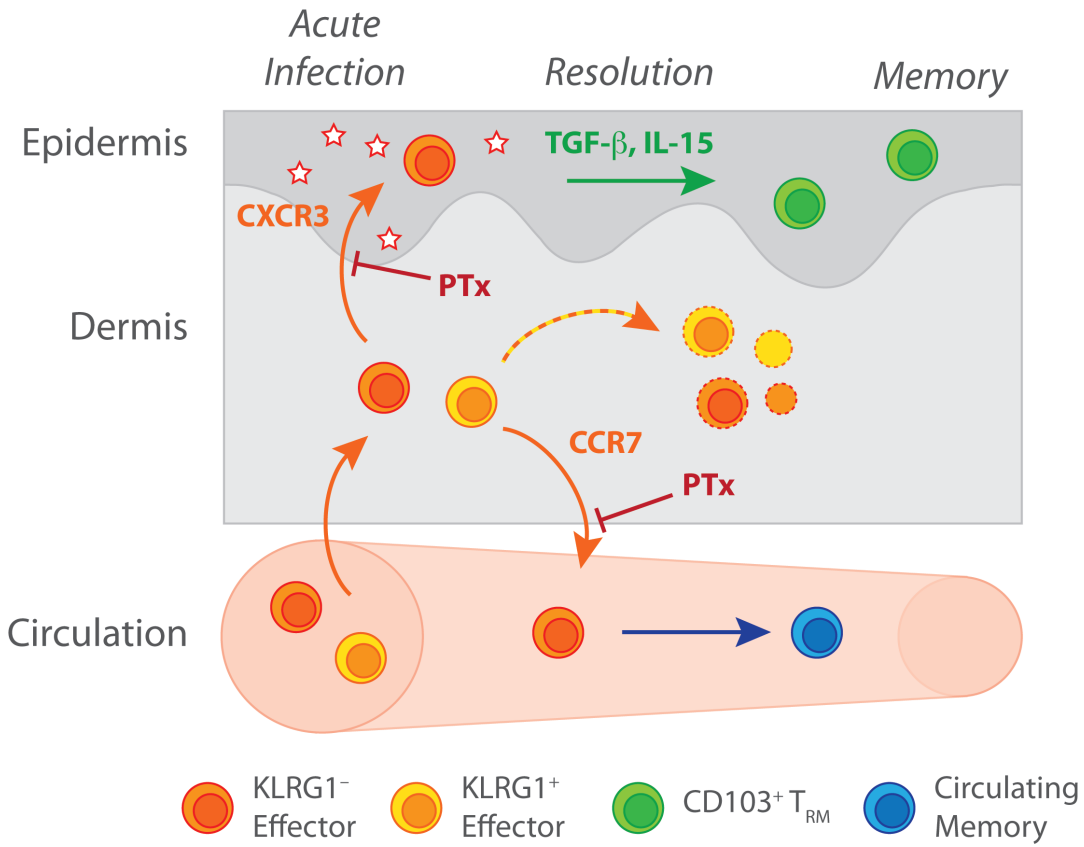

Supplementary Figure 6. The developmental pathway for the formation of T_{RM} cells. KLRG1$^-$ T_{RM} precursors enter the dermis where they may (i) die *in situ*, (ii) exit the skin and return to the blood in a CCR7-dependent manner or (iii) migrate to the epidermis, partly under the influence of CXCR3 ligands. Both tissue exit and epidermal entry are sensitive to treatment with pertussis toxin (PTx) indicating the involvement of G protein-coupled molecules such as chemokine receptors. Following epidermal entry, T_{RM} precursors undergo maturation into long-lived CD103$^+$ T_{RM} cells in a TGF-β- and IL-15-dependent manner. Epithelial T_{RM} cells and their counterparts in the circulation are depicted with different symbols to highlight their distinct transcriptional profiles.

Nature Immunology: doi:10.1038/ni.2744